Optimization of Batch Polymerization Processes—Narrowing the MWD. II. Experimental Study

BRIAN M. LOUIE and DAVID S. SOONG, *Department of Chemical Engineering, University of California, Berkeley, California 94720*

Synopsis

Programmed solvent injection was previously proposed and analyzed in the first part of this two-paper series as a viable alternative for controlling the average molecular weight and narrowing the polydispersity of products from a free-radical polymerization process with an inherent tendency to exhibit strong gel and glass effects. Here, methyl methacrylate is chosen for experimental verification of this idea. The product molecular weight distribution is indeed narrowed.

INTRODUCTION

Solvent addition emerges as the most promising control policy based on our model simulation in Part I, and has thus been selected for experimental verification. Other control strategies have been investigated by previous workers and will not be pursued further here. To validate model predictions, direct experimental observation is needed to prove that the MWD can actually be controlled through programmed solvent addition.

EXPERIMENTAL APPARATUS AND PROCEDURES

A small lab-scale semibatch reactor was constructed to polymerize 500ml of MMA with provision for solvent addition (see Fig. 1). A stirred, 1-L, three-necked distillation flask was used as a reactor. Agitation was provided by a Talboy's Model 120, 1/75 HP, constant torque stirrer with a polypropylene marine-type stirrer operating at about 500 rpm. To prevent oxygen inhibition, a nitrogen blanket was applied across the top of the reactor. Two in-line condensers and an agitator shaft seal were used to minimize the loss of monomer and solvent from the reactor. A 1-gallon water bath was used to provide a well-characterized heat transfer medium. An Omega Model 157-718 PID temperature controller was used to maintain a constant bath temperature. Solvent was metered to the reactor by a Harvard Apparatus #975 syringe pump with a 100-mL syringe. Both reactor and bath temperatures were monitored with a pair of Analog Devices Digital Thermometers #AD2036 interfaced to a Commodore PET 2001 series microcomputer. The temperatures were scanned every 2 min, and the data stored on floppy disks.

Commercial grade methyl methacrylate monomer was obtained from Rohm and Haas Co. The monomer contained 60 ppm hydroquinone inhibitor. Amberlyst A-27 ion exchange resin was used to reduce the inhibitor concentration to 4–10 ppm[1] and the monomer refrigerated prior to use.

Journal of Applied Polymer Science, Vol. 30, 3825–3840 (1985)
 CCC 0021-8995/85/093825-16$04.00

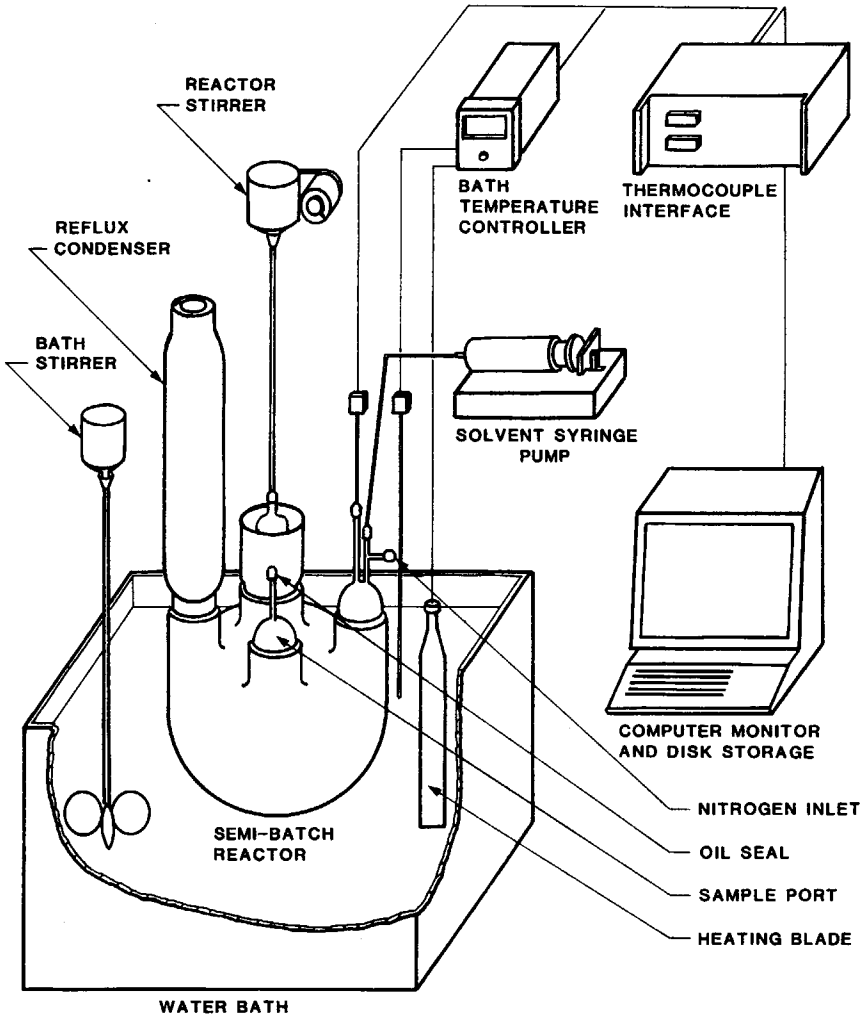

Fig. 1. Schematic of the solution and solvent addition polymerization apparatus. A second in-line condenser and heating blade have been omitted for clarity.

Reagent grade toluene was obtained from Mallinckrodt, Inc. AIBN was obtained from Polysciences, Inc. and refrigerated until use to minimize thermal degradation. House nitrogen was used for the blanket.

At the start of an experiment, the water bath was brought to the desired temperature. All experiments were conducted at 70°C. The monomer (as well as toluene for solution experiments) was then added to the reactor and agitation started. Nitrogen flow was also started to form the blanket. The system was then allowed to stand for 35 min to remove any dissolved oxygen. Afterwards, the AIBN was added in powder form to trigger the polymerization. Because of difficulties in carrying out the exact profile with a syringe pump, the injection profile was approximated by a step pulse.

A sample was taken from the reactor periodically with a 50-mL syringe and placed into a sample bottle containing 10 mL of toluene and trace quantities of 2,2-diphenyl-1-picryl hydrazyl (DPPH) inhibitor. The sample was then quickly cooled in ice to quench the reaction. The cooled samples

were then mixed with about 100 mL methanol to precipitate the polymer. Following evaporation of the methanol and unused monomer, the residues were vacuum-dried to remove any remaining moisture. The polymer was then weighed and the conversion determined. The entire conversion-vs.-time history of the batch was thus delineated.

Number and weight average MWs as well as the MWD were determined with gel permeation chromatography (GPC). Calibration of the GPC columns was done using nearly monodisperse polystyrene and PMMA standards from Pressure Chemicals and Polysciences, Inc. Calibration data based on polystyrene standards were transformed into equivalent PMMA standards by the Universal Calibration method.[2] Standards ranged from 4×10^3 to 2.7×10^6 in molecular weight.

The sample concentration was 0.01% w/v, and all samples were slowly filtered through the 0.45 micro filter provided in Waters Sample Clarification Kit prior to injection into the columns. The typical sample size was 300 μL. Chart speed was about 10.9 cm/min and the solvent flow rate was 2.68 mL/min. Separation efficiency of the GPC columns was above 2000 plates/column and checked periodically during the analysis. No noticeable column degradation and pore plugging were detected.

RESULTS AND DISCUSSION

A set of 12 batch experiments was performed to test our experimental reproducibility and accuracy of model simulations. These simple solution experiments showed that the polymerization does not instantaneously occur upon addition of the initiator. A time lag of almost 10 min is needed to dissolve AIBN into MMA. The reaction rate is apparently retarded initially while the initiator concentration slowly builds up. This leads to lower conversions than those predicted from model simulations. The apparent initiator efficiency is 0.44 over the entire course of reaction. Cause of the initial induction period and low overall initiator efficiency was thought to be due to partially decomposed AIBN after storage in the refrigerator and by trace quantities of hydroquinone inhibitor remaining in the monomer after purification. However, when GPC was performed on some of the polymer samples, lower MWs than those predicted by the model were also found. This is inconsistent with the general belief that higher MWs should be obtained when there is a decreased initiator efficiency or lowered effective AIBN concentration.

Since trace quantities of impurities can have a significant effect on the outcome of our batch runs, small amounts of the ingredients were more carefully purified for further detailed studies. Slightly lower reaction rates were obtained when AIBN was recrystallized from solution and vacuum-dried prior to use. However, when the monomer was vacuum distilled prior to use, almost perfect agreement was reached between experimental data and model simulations (see Table I). Hence, there is a nonvolatile foreign substance in the monomer acting as a chain transfer agent

$$P_n\cdot + F \xrightarrow{k_1} D_n + F\cdot$$
$$F\cdot + M \xrightarrow{k_2} F + P_1\cdot$$

TABLE I
Effects of Monomer and Initiator Purification on the Isothermal Bulk Polymerization of MMA

Exptl conditions	Exptl X (%)	Exptl $\overline{M}_n$	Exptl $\overline{M}_w$	Exptl HI
CSTR with agitation in air at steady state				
T = 80°C, [I] = 0.0268M AIBN				
Undistilled MMA and unpurified AIBN	8.9	26K	48K	1.85
Theoretical	22.5	78K	155K	1.99
BATCH without agitation				
T = 80°C, [I] = 0.0067M AIBN				
Undistilled MMA and purified AIBN	5.65	111K	211K	1.90
Distilled MMA and unpurified AIBN	4.2	132K	253K	1.92
Theoretical	5.0	156K	312K	1.99
BATCH without agitation				
T = 80°C, [I] = 0.0067M AIBN				
Undistilled MMA and unpurified AIBN	4.9 at 10.25 min			
Undistilled MMA and recrystallized AIBN	5.5 at 10.6 min			

where F is the foreign substance (probably short chain oligomers formed by the hydroquinone in the inhibition process), and k_1 and k_2 are radical transfer rate constants. Retardation of the polymerization occurs when $k_2 << k_1$. This would explain both the low conversions and low MWs found experimentally.

Since it is not feasible to scrupulously cleanse the monomer of impurities and inhibitors for a large-scale industrial process, the model was slightly modified to account for the above findings. The experimental initiator efficiency is used instead of the theoretical value of 0.58 and chain transfer to monomer (which can embody transfer to oligomers) is adjusted to bring the MWs into agreement (see Fig. 2). Chain transfer must be increased 20-fold from that estimated by the correlation of Stickler and Meyerhoff.[3] However, this value is not unreasonable when compared to the scatter of chain transfer coefficients reported for MMA in the literature (see Fig. 3). Monomer conversion predictions are shifted to right of the ideal model curve due to the adjustment of initiator efficiency.

Figure 4 shows some of the experimental data when compared to the modified model simulations. Good agreement is reached prior to reactor runaway. Experimental conversions and temperatures are higher than those predicted by the model at moderate conversions, due to nonideal mixing (segregation) at high viscosities. Reactor contents then separate into circular layers which spin around the agitator at different speeds. Faster rates (due to autoacceleration occur in the outer layers as local polymer concentrations rise. This leads to the higher cup-mixed (measured) coversions. Reactor volume shrinks when conversion in the outside layer reaches the point where a polymer gel forms. Thermal runaway soon follows as the gel layer grows and severely hinders heat transfer.

Solvent evaporation may play an important role in causing discrepancies between model predictions and experimental results, especially at low sol-

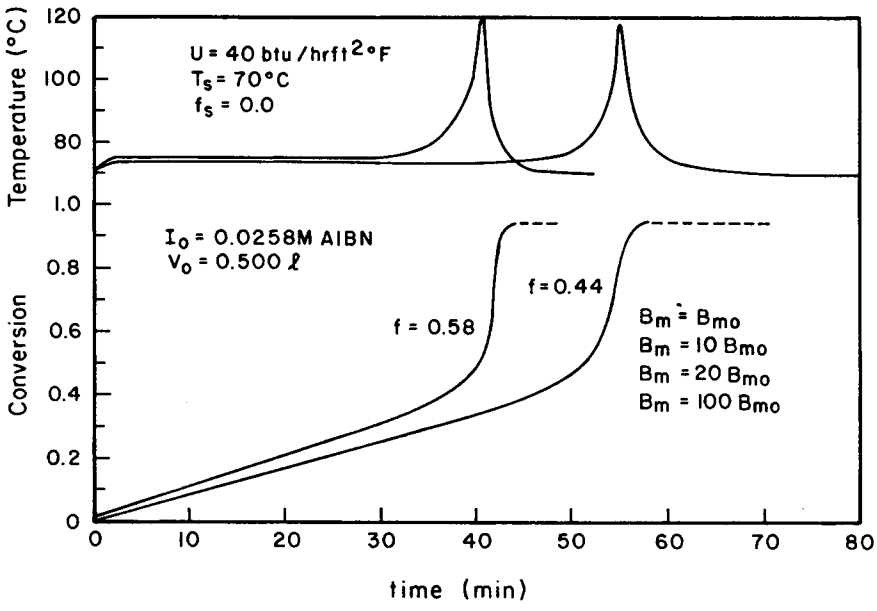

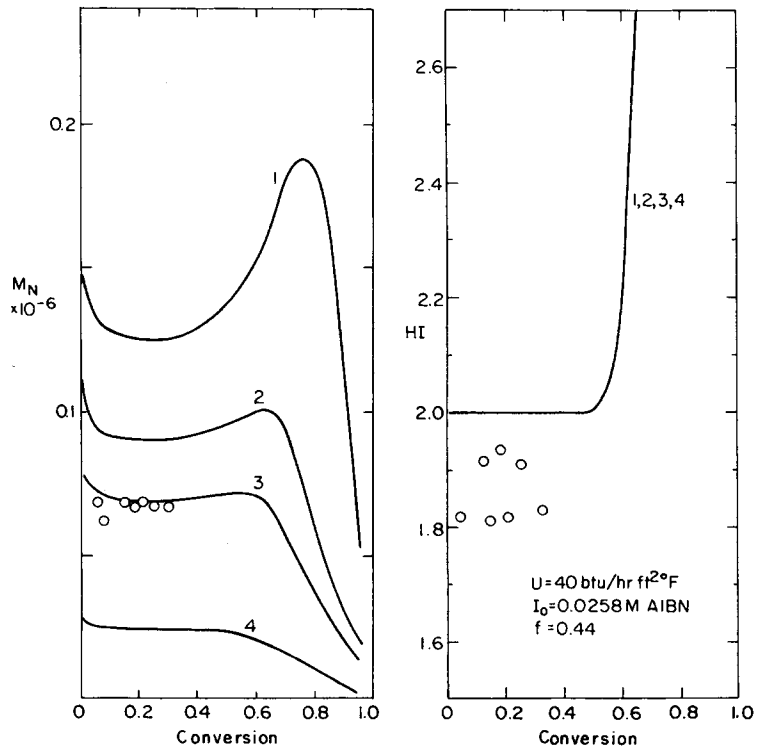

Fig. 2. Retardation in the polymerization of MMA is modeled by adjusting the initiator efficiency and the transfer constant to monomer, B_m (or k_f/k_p). Bottom: (○) experimental data; $B_m = B_{m0}$ (1), 10 B_{m0} (2), 20 B_{m0} (3), 100 B_{m0} (4), where B_{m0} is computed from the correlation of Stickler and Meyerhoff.[3]

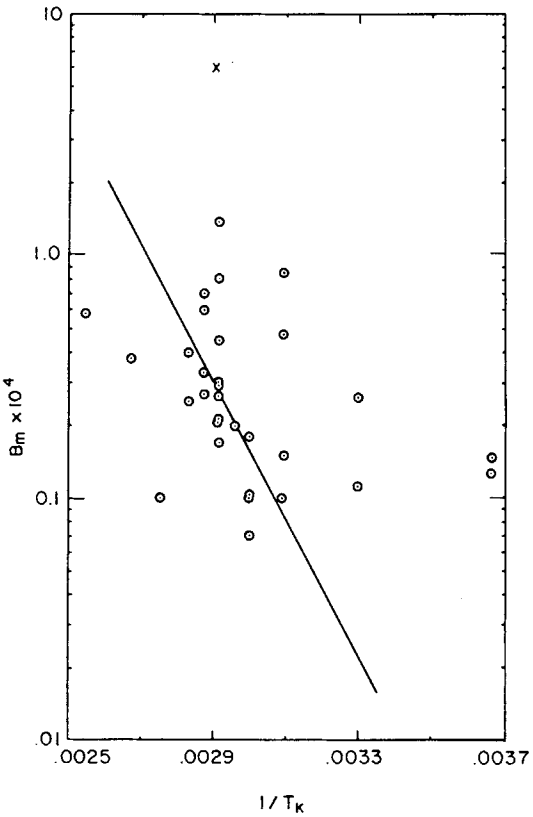

Fig. 3. Comparison of reported transfer constants to monomer with the correlation of Stickler and Meyerhoff[3] and our experimental observation. Much of the scatter is probably due to either dissolved oxygen or trace impurities not removed by monomer distillation: $B_m = 9.48 \times 10^3 \exp(-13380/RT_k)$; (X) our experimental result; (○) data of *Polymer Handbook.*

vent fractions. This is probably the case for $f_s = 0.2$ (see Fig. 4). At $f_s = 0.4$, reaction rates are sufficiently slow to avoid boiling off the solvent. Experimental conversion is slightly less than the predicted level because of partial oxygen inhibition. Atmospheric oxygen is introduced into the reactor at moderate conversions because the sample port must be opened longer to allow the viscous polymer to be sampled. A sample may be withdrawn in 15 s when the conversion is less than 10%, but 5 min may be needed per sample above 30% conversion. Small dips in the reactor temperature were also noted during sampling.

A curious observation from the solution experiments is noted when the experimental PD is compared to the predicted PD (also see Figs. 5 and 6):

f_s	x	Exptl HI	Calcd HI
0.0	17.7	1.94	1.98
0.2	18.8	1.80	1.98
0.3	18.1	1.60	1.98
0.4	23.3	1.55	1.98
0.5	18.2	1.51	1.98

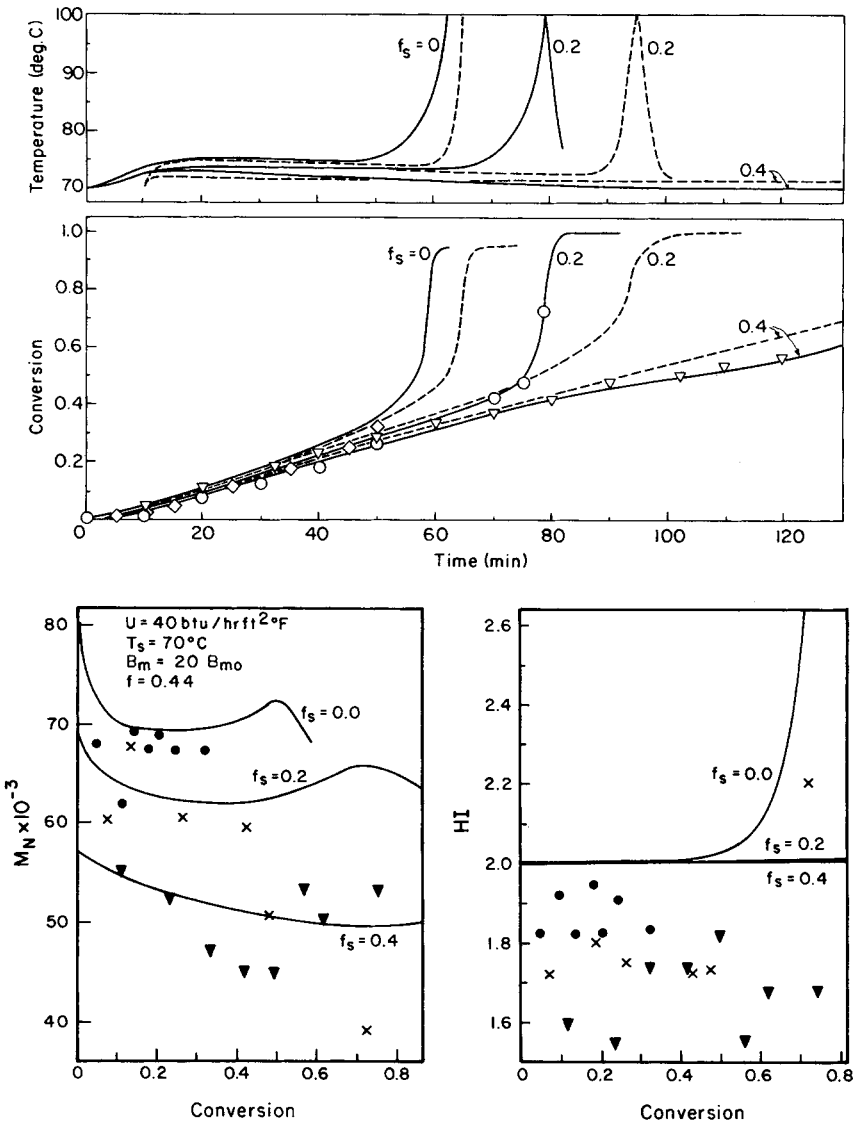

Fig. 4. Experimental data and model predictions with retardation accounted for. Experimental conversions (—, ●, ▼) and theoretical predictions (- - -) show good agreement until thermal runaway occurs. Good agreement is also reached for MW, but HI is overpredicted. Solvent fraction (date of expt): (◇, X) 0.0 (7/23/83); (○, ●) 0.2 (7/24/83); (▽, ▼) 0.4 (6/16/83).

As the solvent fraction increases, the MWD narrows. A faulty GPC column would have led to peak broadening, while random error would have produced scatter in the data. These experimental MWDs are narrower than the theoretical PD and definitely support a change in the mode of termination. This observation is supported by Figure 7, which shows that narrowing does not occur until solvent is added. It also eliminates the possibility that the discrepancy is due to a systematic error (such as from consistent clipping of the low MW tail in our GPC traces).

The only likely explanation is that the ratio of disproportionation to combination, k_{td}/k_{tc}, is solvent-fraction-dependent (with k_{td}/k_{tc} decreasing

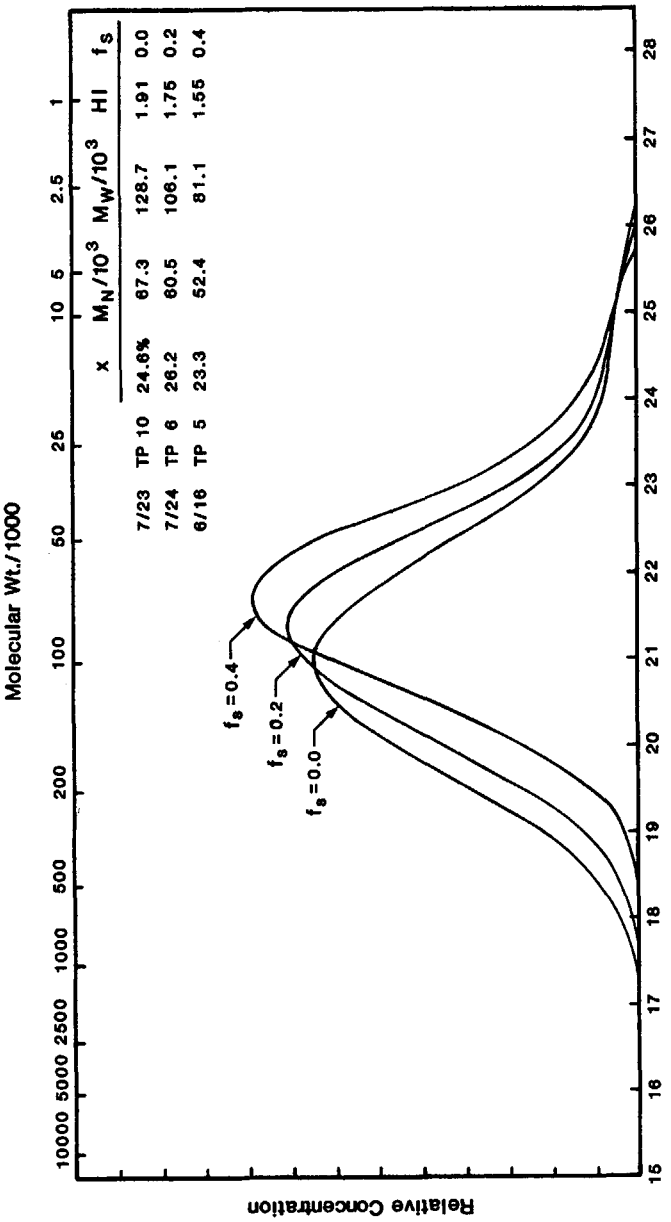

Fig. 5. Experimental GPC traces as a function of solvent fraction. Narrower MWDs are obtained at higher solvent fractions.

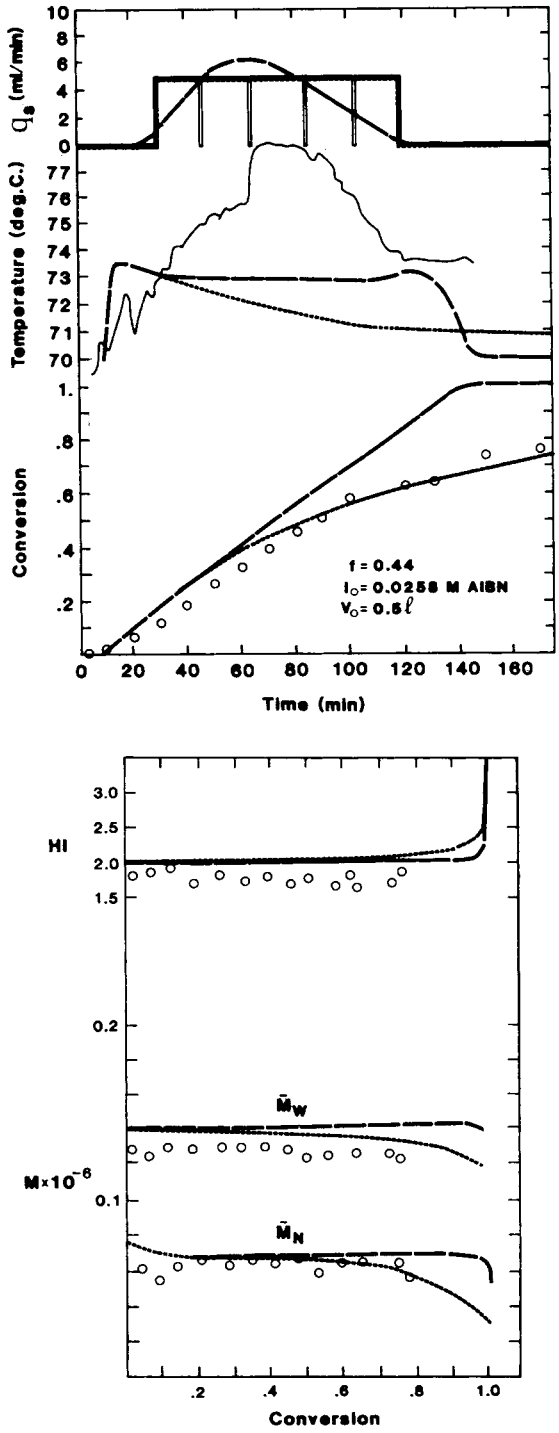

Fig. 6. Comparison of the experimental step pulse with the simulated step and optimum (minimum HI) solvent profile. Good agreement is obtained between the experimental data and model predictions. The actual step overadds the minimum amount of solvent, but this does not appear to affect MW and HI until high conversion is reached: (. . .) step pulse; (— —) optimum addition; (—, ○) exptl.

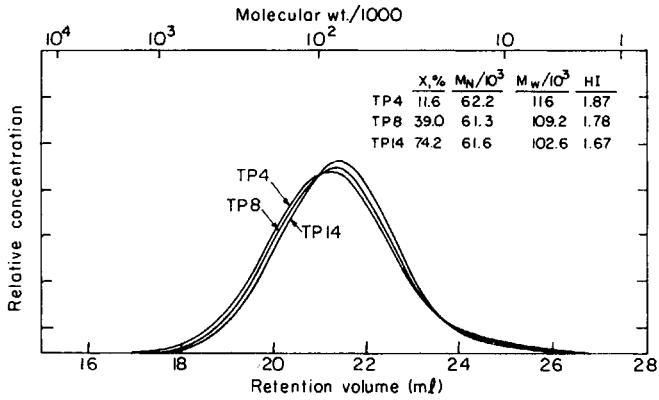

Fig. 7. Experimental GPC traces obtained during the solvent step-pulse experiment. MWD narrowing does not begin until solvent addition has started, suggesting that k_{td}/k_{tc} is solvent-dependent.

with increasing solvent fraction). This is possible because the hydrogen abstraction reaction required for termination may be more favorable as the viscosity decreases. However, this idea is not supported by the literature data. When Bevington et al.[4] originally studied MMA polymerization to determine k_d/k_{tc}, the reaction was carried out in 50% benzene and no solvent effects were noted (i.e., they predicted a PD = 2). We are thus puzzled by our observation. More work is clearly needed because smaller PDs may be produced by adding more solvent. This would then have a tremendous effect on the optimum solvent addition profile.

Four solvent step-addition runs were performed at 70°C with 0.0258*M* AIBN. Details of the step-pulse programs and the experimental outcome are listed below.

Experiment no.	Pulse flow rate (mL/min)	Start time (min)	Stop time (min)	Result
1	3.7	40	End of expt	Thermal runaway
2	3.7	35	End of expt	Thermal runaway
3	5.2	30	120	Successfully controlled
4	7.3	35	End of expt	Reaction stopped

Adding too little solvent results in an uncontrollable reaction, while adding too much solvent almost completely stops the polymerization (via monomer and initiator dilution). These results indicate that a narrow window of experimental solvent pulses exists because the solvent is not mixed rapidly enough in our experiments.

Figure 7 compares the experimental conversion history, temperature evolution, solvent injection profile, and molecular weights for run 3 with model predictions of the experimental and optimum solvent pulses. The actual solvent flow was periodically interrupted to refill the solvent syringe. Thus the total solvent pulse was actually divided into several smaller pulses. The experimental rate of polymerization is lower than that corresponding to the optimal injection profile because more than the optimum amount of solvent has been added. Experimental conversion and MWs are in good agreement with simulations for a step pulse program.

Small temperature fluctuations occur whenever a sample is withdrawn from the reactor, and are most prominent at low conversions. Around 60 min, it was discovered that the reactor thermocouple was in direct contact with the incoming solvent stream. Redirecting the solvent flow to another location resulted in a sudden rise in recorded temperatures. Earlier recorded temperatures are then in slight error due to solvent cooling. Temperatures fall slowly when enough solvent has been added to reduce the rate of heat generation below the rate of heat removal. A large discrepancy exists between the experimental and theoretical temperature profile because a thin viscous polymer layer was found on the inside walls of the reaction flask when the reactor contents were emptied. This layer reduced heat transfer significantly and was primarily responsible for the elevated temperature. This effect cannot be compensated for because the overall heat transfer coefficient is an unknown function of time. (A single U_{avg} does not suffice.) Solvent cooling probably prevented reactor runaway in experiment 3.

The narrow scatter of MW data confirms that an almost constant kinetic chain length can be maintained throughout most of reaction. This kept PD under tight control. A slight narrowing of the MWD occurred at high conversions as the solvent fraction increased (see Fig. 7). This is consistent with our earlier solution results that solvent narrows the MWD. The final product PD was then less than the predicted PD.

More solvent-addition experiments were not performed because the results appear to be very sensitive to the homogeneity of the reacting mixture and to how fast the solvent could be mixed into solution. Experimental data are not likely to be reproducible unless identical mixing conditions are employed. Thus, only a feasibility demonstration that solvent addition can control the MWD is needed. More powerful mixers and better solvents should improve the process. Careful attention to reactor mixing is clearly recommended for scaling up a solvent addition, semibatch reactor.

SENSITIVITY OF THE OPTIMUM PROFILE TO THE GEL EFFECT MODEL

An important question concerning solvent addition is the sensitivity of the optimum solvent profile to the constitutive equation chosen to describe the gel effect. Only one model, the CCS model, has been used thus far. The spread in predicted behavior using six other contemporary constitutive equations for the gel effect was also studied. These equations can be found in a previous publication.[5] Mainly single population models have been simulated, but the COD model was included to represent multiple population

models (see Figs. 8–10). Most of the models predict similar conversion, molecular weight, and polydispersity profiles. However, the optimum solvent injection histories are vastly different depending on the particular gel effect equation used.

Since these gel effect models were derived with different assumptions and sometimes slightly different rate constants, a direct comparison of the various solvent flow profiles is not possible. However, the general behavior—the shape and number of solvent peaks—will remain unchanged. No

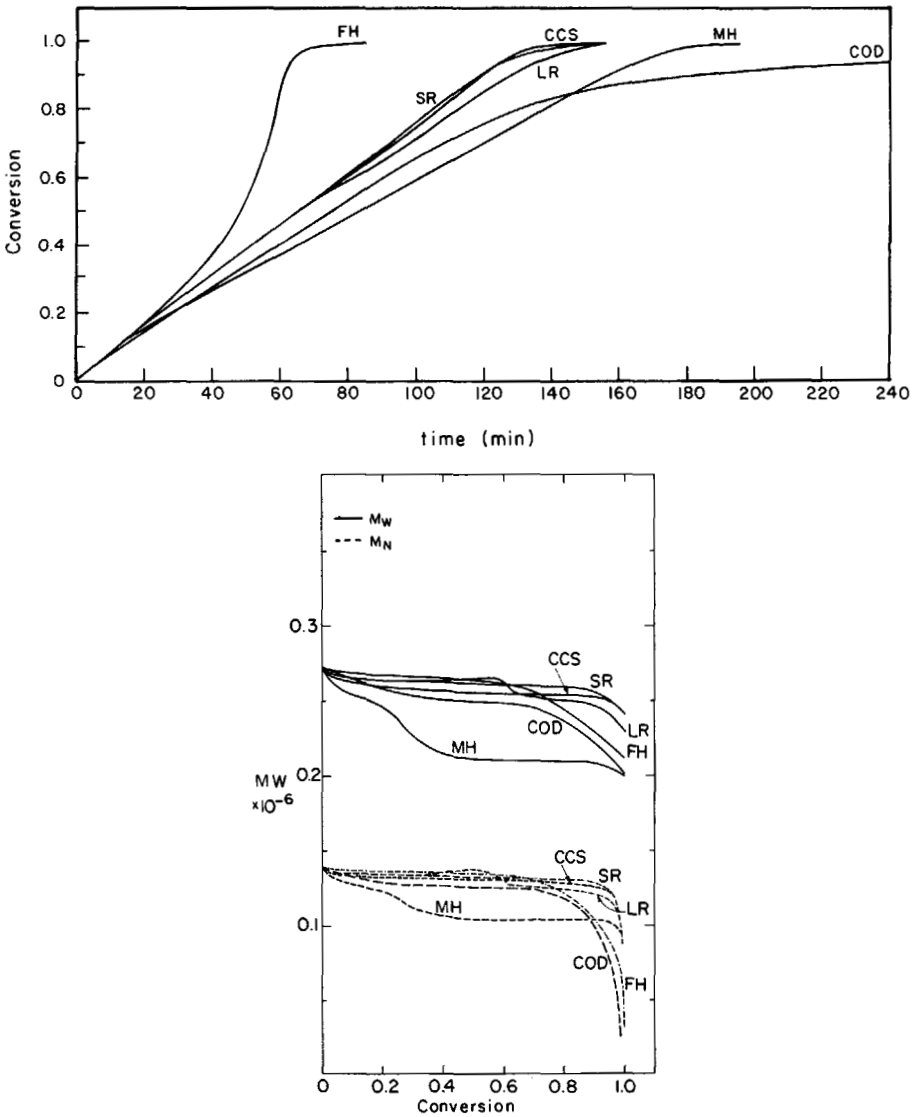

Fig. 8. Dependence of the optimum isothermal solvent addition policy on the gel effect model used: (FH) Friis and Hamielec (1973); (MH) Martin and Hamielec (1978); (LR) Ross and Laurence (1976); (SR) Schmidt and Ray (1981); (COD) Cardenas and O'Driscoll; (CCS) Chiu, Carratt, and Soong (1983). (T = 70°C, $[I_0]$ = 0.0258M AIBN, V_0 = 0.5 L.)

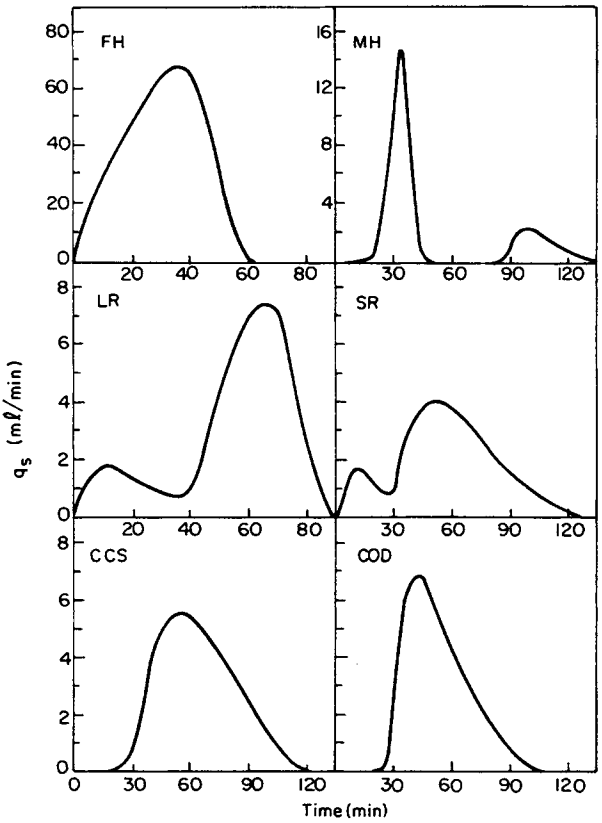

Fig. 9. Comparison of the optimum solvent addition profile produced by using different gel effect models: (FH) Friis and Hamielec (1973); (MH) Martin and Hamielec (1978); (LR) Ross and Laurence (1976); (SR) Schmidt and Ray (1981); (COD) Cardenas and O'Driscoll; (CCS) Chiu, Carratt, and Soong (1983).

one gel effect model is generally accepted, but the MH, SR, COD, and CCS models have been specifically tested for solution polymerization. Reasons for the sensitivity of the optimum are discussed below.

The Friis and Hamielec (FH) model is an empirical gel effect model that does not incorporate an explicit solvent dependence. MW, and hence PD, can only be controlled through chain transfer to solvent. Since the gel effect begins right at the start of polymerization (see Fig. 10), very large quantities of solvent must be added even at low conversions. This solvent later pulls down the number average molecular weight at high conversions and raises the product polydispersity.

The Ross and Laurence (RL) and Schmidt and Ray (SR) models both predict two solvent peaks. Insight into the nature of the peaks can be obtained from studying the termination rate constant for bulk polymerization (see Fig. 10). k_t falls slowly in response to segmental diffusion until the onset of the gel effect where translation diffusion control begins to dominate. Both SR and LR models represent this transition as a break point. Since a constant termination rate is desired to control the PD, the first solvent peak is added to minimize the initial drop while the second peak is needed

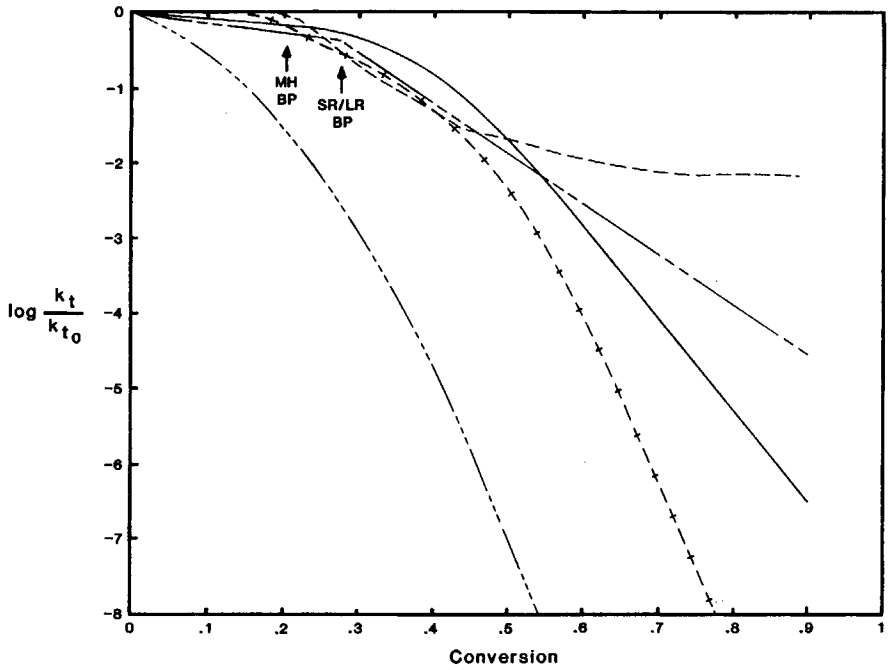

Fig. 10. Various model predictions for the apparent termination rate constant for the bulk polymerization of MMA. Models with break points tend to require multiple solvent additions: (FH) (—- - -—) Friis and Hamielec (1973); (MH) (— +) Martin and Hamielec (1978); (LR) (—- -—) Ross and Laurence (1976); (SR) (—- -—) Schmidt and Ray (1981); (COD) (—) Cardenas and O'Driscoll; (CCS (—) Chiu, Carratt, and Soong (1983).

to surpass the break point when the onset occurs. Failure to clear the break point results in broadening of the MWD. Less solvent is needed for the SR model than the RL model, because of a stronger free volume dependence on the solvent.

The Martin and Hamielec (MH) model also shows two distinct peaks, as this model also has a break point. Since segmental diffusion control was neglected in this model, no solvent is required until the critical break point condition is reached. Since this condition is mainly dependent on the weight average MW, a large pulse of solvent is needed to dilute the polymer to prevent it from forming entanglements. This solvent slows the polymerization rate and drops the MWs. A second smaller peak occurs later when another critical condition is reached. Less solvent is needed now as large quantities are already present.

Only a single solvent peak is predicted by the Cardenas and O'Driscoll (COD) and the Chiu, Carratt, and Soong (CCS) models because both employ continuous functions to represent kinetic rates (see Fig. 10). The primary difference between the two models lies in the amount of solvent needed to control the gel effect. In the CCS model, the gel effect is treated as a free-volume, diffusion-limitation effect. Only enough solvent is added to improve macroradical mobility by opening voids in the solution to allow for diffusion. In the COD model, polymer entanglements cause the gel effect. Thus, more

solvent is needed to dilute the concentration of dead chains, and not just to open voids. This extra solvent causes MWs to fall sooner than predicted by the CCS model. Reaction rates are also slightly lowered. This illustrates that model sensitivity to MW is important and must be incorporated in future studies.

The model of Tulig and Tirrell (1981) was also simulated, but answers could not be obtained beyond the first break point. This is because the model has specific dependences on both the concentration of polymer and number average MW. Optimization will strongly depend on prior polymerization history. Results were obtained with the MH model because the break point was mainly sensitive to the free volume. With the TT model, several local minima may exist since k_t is sensitive to both MW and polymer concentration. This optimization problem could not be solved within 2.5 CPU min on the IBM 4341 and the run was aborted. Their model contains two break points so that it is conceivable that two solvent peaks would be present in their optimum profile.

Preference of gel effect models cannot be gleened from our experimental results. The solvent step pulse used could easily approximate most of the models proposed. Thus, no firm conclusions can be reached concerning the most accurate optimum solvent profile. Nonideal mixing further complicates interpretation of experimental results. This prevents experimental determination of the optimum solvent addition profile. In this work, we have acquired the tools for optimizing solvent addition, but further progress must wait until a clearer understanding of the gel effect is available.

CONCLUSIONS

Most previous experimental and theoretical studies have focused on styrene polymerization because of its commercial importance. However, styrene does not exhibit a strong gel effect so that the effects of diffusion-controlled termination on the optimal control policy have not been fully appreciated. This is true of the minimum end-time problem, where dead-ending or constant initiation rates have been proposed, but appear to yield higher polymer polydispersities than those obtained when the minimum MWD policy is followed. By not narrowing the MWD, the polymer produced may not adhere to specifications.

This study differs from past works in its attention to the details of the reaction kinetics, whereas others have focused primarily on the optimization. The gel and glass effects, volume expansion and contraction, radical accumulation, and other phenomena have been included. The optimum temperature and initiation histories along with monomer and solvent addition profiles for isothermal and nonisothermal semibatch PMMA reactors have been determined. Of these methods, selective solvent addition has been shown to be quite promising in controlling the MWD to complete conversion. Good agreement was found between experimental results and model simulations. However, design and optimization of such reactors is severely hampered by our poor understanding of reactor mixing and the gel effect. More work in this area is needed.

References

1. L. S. Luskin, in *Vinyl and Diene Esters, Vol. XXIV, High Polymers,* C. E. Schildknnecht and I. Skiest, Eds., Wiley-Interscience, New York, 1965, p. 105.
2. A. Ouano, *J. Macromol. Sci.,* **C9**(1), 123 (1973).
3. M. Stickler and G. Meyerhoff, *Macromol. Chem.,* **179**, 2729 (1978).
4. J. C. Bevington, H. W. Melville, and R. P. Taylor, *J. Polym. Sci.,* **14**, 463 (1954).
5. B. M. Louie and D. S. Soong, *J. Polym. Sci.,* to appear.

Received September 20, 1984
Accepted January 18, 1985